Chapter 3:
Movement of Deep-Sea Coral Populations on Climatic Timescales

3.1 ABSTRACT

During the past 40,000 years global climate has moved out of a full glacial period, with the deglaciation marked by several millennial scale rapid climate change events. Here we investigate the ecological response of deep-sea coral communities to both glaciation and rapid climate change. We find that the deep-sea coral populations of *D. dianthus* in both the North Atlantic and the Southern Ocean expand at times of rapid climate change. However, during the more stable Last Glacial Maximum the coral population globally retreats to a more-restricted depth range. Holocene populations show regional patterns that provide some insight into what causes these dramatic changes in population structure. The most important factors are likely responses to climatically driven changes in productivity, $[O_2]$ and $[CO_3^{2-}]$.

3.2 INTRODUCTION

The role of the deep ocean in climate change has been a central theme of paleoceanography from the early days of the field. As the locus of nearly all the mass, thermal inertia, and carbon in the ocean-atmosphere system, the deep ocean's overturning rate is a crucial parameter in understanding past climates. Probing the distributions and rates of deep-water mass shifts during times of past climate change has largely been informed by geochemical tracers. For instance, the distribution of $\delta^{13}C$ (Curry and Lohmann 1985; Raymo, Ruddiman et al. 1990) and Cd/Ca (Boyle and Keigwin 1982; Oppo and Horowitz 2000) in the water column during glacial periods shows that the volume of southern source waters in the Atlantic increases at the expense of northern source waters. Recently, one of the most promising of these tracers has been radiocarbon as it has an internal clock intrinsic to the tracer. In the modern ocean the deficit of the $^{14}C/^{12}C$ ratio in the ocean interior, as compared to its production by cosmic rays in the atmosphere, is one measure of the ventilation rate of the deep-sea. In the past ocean combined U-series and ^{14}C ages,

and benthic minus planktonic ^{14}C ages, have been able to constrain the rate of deep ocean overturning.

However, as successful as the geochemical tracers have been, the distribution of benthic foraminifera species was actually one of the first indicators of deep ocean change (Streeter and Shackleton 1979). Streeter and Shackleton noticed that *Uvegerina peregina*, a benthic foraminifera which is correlated with the distribution of Antarctic Bottom Water (AABW), was abundant in LGM sediments that are today bathed by North Atlantic Deep Water (NADW). The authors hypothesized, correctly, that southern sourced waters replaced NADW as the dominant abyssal water mass in the LGM Atlantic and suggested that North Atlantic deep water production was much reduced. Using species distributions in space and time to constrain aspects of the physical climate was epitomized in the CLIMAP program. CLIMAP was a successful effort to map surface populations of foraminifera during the Last Glacial Maximum (LGM) and to attribute the changing populations to variations in sea surface temperature. In this paper we show how the combination of these two types of research, geochemical and faunal constraints on past ocean behavior have come together in the study of deep-sea corals in the North Atlantic and Southern Oceans. We show how coral population changes in space and time are like the deep ocean version of CLIMAP and reveal remarkable correlations with climate.

Deep-sea corals are a relatively new archive in paleoclimate. Our preferred species *Desmophyllum dianthus* is uranium rich, visually banded, and grows for decades to 100 years. Like all scleractinians it can also be precisely U-series (Cheng, Adkins et al. 2000) and radiocarbon dated (Robinson, Adkins et al. 2005) . This combination of precise, independent calendar ages frees ^{14}C from being a chronometer and allows us to measure the past ocean $\Delta^{14}C$ content as recorded in the coral skeleton. Combined with the potential for unbioturbated decadal resolution records of deep ocean change, deep-sea corals are a unique and powerful archive of past geochemical information. Previously, the use of deep-sea corals to solve problems in paleoclimate was chiefly limited by their perceived paucity on

the sea floor. However, recent work has demonstrated that several genera of deep-sea corals have a global distribution (Cairns 2007), making them ideal candidates for constraining the intermediate and deep ocean's role in climate change. A recent census of azooaxanthellar corals revealed that there are at least as many species of 'deep-sea coral' as there are surface corals (Cairns, 2007).

Since 2003 we have made a systematic effort to collect fossil deep-sea corals from two regions each near a site of modern deep-water formation. In several cruises with the deep submergence vehicle Alvin and the remotely operated vehicle (ROV) Hercules, we collected more than 5,000 fossil *D. dianthus* individuals from the New England (34–40°N, 60–68°W) and Corner Rise Seamounts (34–36°N, 47–53°W). We also collected more than 10,000 fossil *D. dianthus* samples from south of Tasmania (43–47°S, 144–152°E) in 2008 and 2009 using the ROV Jason. Collection by ROV and submarine ensures that the depth of each coral is precisely known and that corals are collected near their paleo growth position. At the time of collection we know the latitude, longitude, and depth of the coral's growth, but we have no idea about when it grew.

Unlike sediment cores where an age model can be constructed by extrapolating between dates made on foraminifera, every individual deep-sea coral sample must be dated prior to being used for paleoclimate analysis. In this work, we take advantage of a new development, the reconnaissance dating method at WHOI's accelerator mass spectrometry facility (NOSAMS), to radiocarbon date more than 500 of these *D. dianthus* samples. We construct, for the first time, the history of benthic population movements in space and time since the last glacial period. This effort is similar to an ostracod dataset from the deep North Atlantic that demonstrated that the Pliocene ostracod species diversity is related to changes in solar insolation caused by changes in Earth's obliquity (Cronin and Raymo 1997). However the combination of Reconnaissance radiocarbon dating and deep-sea corals has allowed us to rapidly and inexpensively construct an extensive dataset of a species' habitat preferences. Rather than having to work up many sediment cores across a depth range,

our search for deep-sea coral samples that grew during times of rapid climate change has produced a view into benthic ecology on long timescales. We present the largest record to date of changes in the deep-sea coral distributions in the North Atlantic and Southern Ocean for the last 40,000 years. Our sample set is large enough to capture the temporal resolution necessary to see rapid climate change events in both hemispheres. This record (Figure 3.1) provides an unprecedented view of the deep-sea ecological response to climate change. In addition, this paper's use of radiocarbon dating in an 'age screening' mode demonstrates how recent analytical advances can dramatically change the way ^{14}C dates are used in paleoclimatology and paleoecology.

3.3 METHODS AND MATERIALS

We collected more than 5000 *Desmophyllum dianthus* from the New England (34–40°N, 60–68°W) and Corner Rise Seamounts (34–36°N, 47–53°W) in 2003–2005 using the deep submergence vehicles ALVIN and HERCULES. We also collected more than 10,000 *Desmophyllum dianthus* from south of Tasmania (43–47°S, 144–152°E) in 2008 and 2009 using the deep submergence vehicle JASON. Collection by ROV and submarine ensured that the depth of each coral was precisely known and that corals were collected near growth position.

Ninety-five corals from the New England and Corner Rise Seamounts and two hundred and forty-nine corals from the Southern Ocean were selected randomly from our collection across seamounts and depths for ^{14}C analyses. There is some possibility for a size bias as whole corals rather than fragments were used.

Corals were dated using a reconnaissance dating method involving an elemental analyzer and sealed tube zinc reduction method for preparing graphite (Xu, Trumbore et al. 2007; Burke, Robinson et al. 2010). This method allowed for many more samples to be dated at a much lower cost than traditional hydrolysis methods.

3.3.i. Radiocarbon Method

Samples of 8–15 mg were taken from each coral and physically and chemically cleaned to remove the ferromanganese crust that was coating it (Adkins, Griffin et al. 2002).

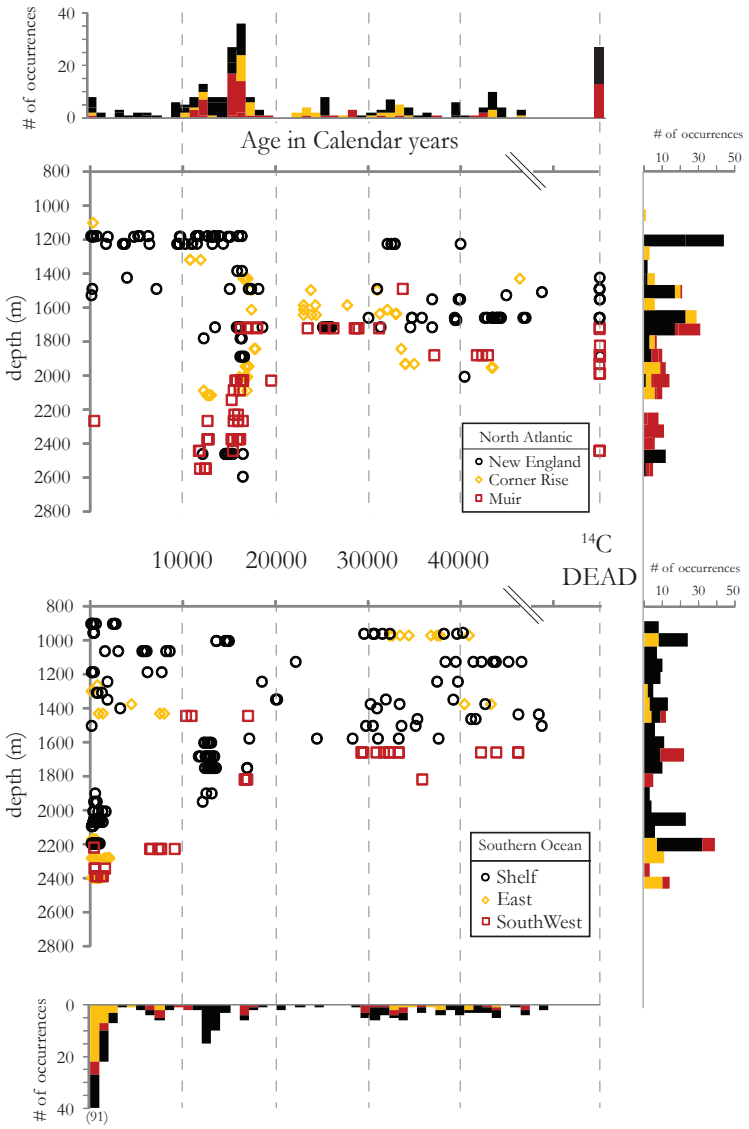

Figure 3.1: The age-depth distributions of deep-sea corals from the North Atlantic and Southern Ocean seamounts for the past 50,000 calendar years. These corals were dated using the reconnaissance dating method (and then converted to calendar age (see SOM for details) and U/Th (22). Each point represents a single age from a single *D. dianthus* coral. The histograms above and below the plots represent the number of corals for each 1000 year age bin. The histograms at the side of the plot represent the number of corals for each 75 m depth bin. Corals were collected from 1098-2740 m (while searching from 900-2800 m) in the North Atlantic and from 898-2395 m (while searching from 898-4000 m) in the Southern Ocean. The break in the age axis demonstrates that there is a population of corals that are 14C-dead in the N. Atlantic but not in the Southern Ocean.

Corals from 2009 were physically cleaned using a Dremel tool and a sandblaster and then chemically washed with MeOH which had been shown to be equivalent to the more labor intensive cleaning done in 2008 (Burke, Robinson et al. 2010). Corals were then combusted in an EA and the resulting CO_2 from combustion was extracted cryogenically on a vacuum line attached to the EA. The CO_2 was frozen into a reaction tube which contained Zinc and Titanium hydride and Fe catalyst. The sample was then graphitized in a furnace for 3 hours at 500°C and 4 hours at 550°C, and analyzed for Fm at The National Ocean Sciences Accelerator Mass Spectrometry Facility at Woods Hole Oceanographic Institute.

Coral standards were run using the traditional hydrolysis method and the reconnaissance dating method to ensure that there was no bias to the reconnaissance dating method (Figure 3.2). Coral standards were also run at regular intervals during sample processing (Figure 3.3).

We converted all radiocarbon dates to calendar ages by applying four different constant offsets during four time periods. We used the modern age of the water column in the North Atlantic (600 years) and Southern Ocean (1250 years) to make a reservoir correction for all Holocene data. We used the ^{14}C age and U/Th age difference (1500 years) as measured in corals from the New England Seamounts during the Younger Dryas to convert Younger Dryas measurements(Robinson, Adkins et al. 2005). For all other corals during the glacial time period in the North Atlantic we used the ^{14}C age and U/Th age difference (1000 years) measured in Heinrich 1 corals to make a reservoir (Robinson, Adkins et al. 2005). For all glacial corals in the Southern Ocean we used the average of the ^{14}C to U/Th age difference (1900 years) measured in the ACR (Table 3.4) to make a reservoir correction. We converted all ^{14}C dates to calendar ages using Intcal09 and the Calib 6.0 software.

After analyzing the 344 ^{14}C Reconnaissance measurements, 80 more corals were randomly selected from 1375–1575 m water depth from the Southern Ocean to improve the population statistics of intermediate water column coral distributions (Figure 3.4).

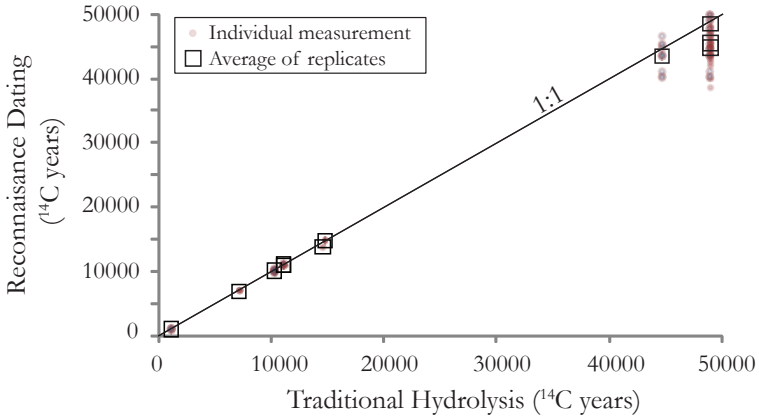

Figure 3.2: Comparison of reconnaissance dating method versus hydrolysis dating.

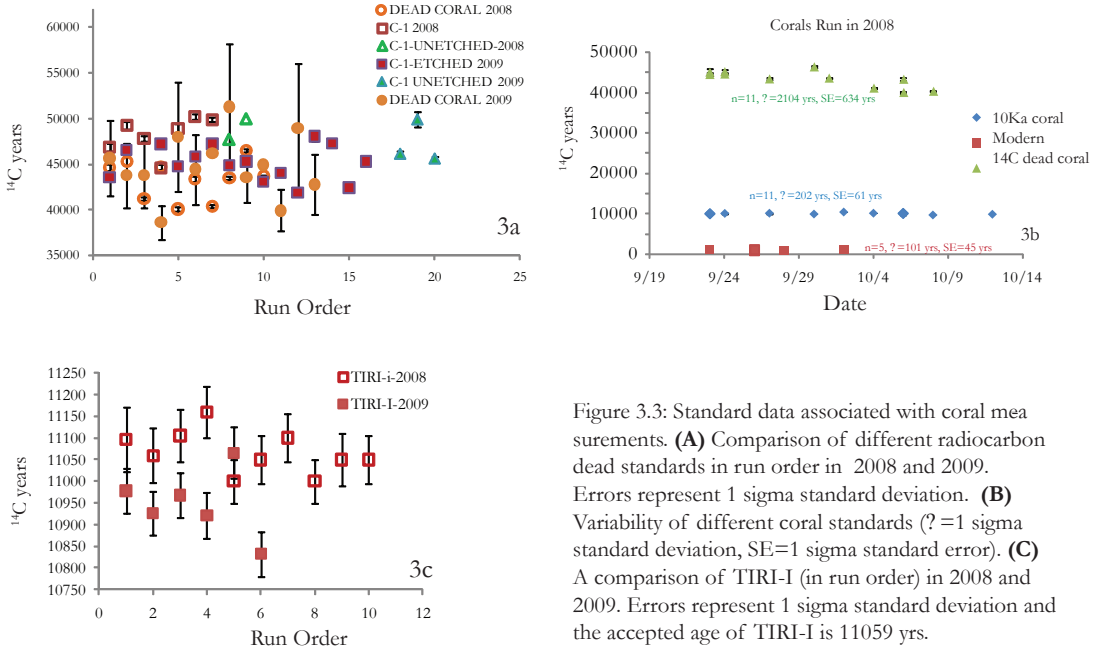

Figure 3.3: Standard data associated with coral mea surements. **(A)** Comparison of different radiocarbon dead standards in run order in 2008 and 2009. Errors represent 1 sigma standard deviation. **(B)** Variability of different coral standards (? =1 sigma standard deviation, SE=1 sigma standard error). **(C)** A comparison of TIRI-I (in run order) in 2008 and 2009. Errors represent 1 sigma standard deviation and the accepted age of TIRI-I is 11059 yrs.

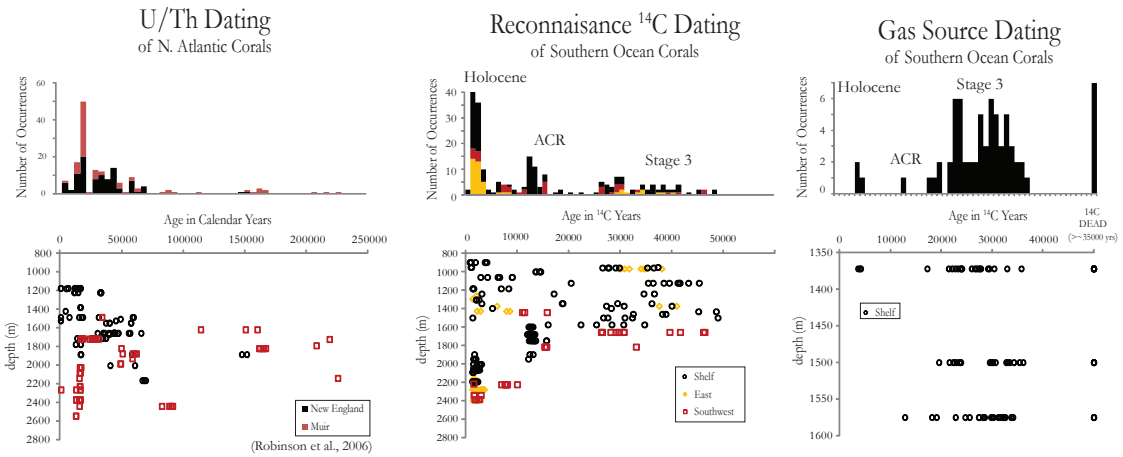

Figure 3.4: This figure describes the various methods of dating corals. The U/Th method can be used to screen corals up with an age of ~ 500,000 calendar years. This process is more labor intensive than ^{14}C dating. A ^{14}C date gives the age of the DIC from which the coral precipitated from as opposed to calendar years. Traditional hydrolysis ^{14}C dating is more time consuming and expensive; however, there are two new ^{14}C dating methods that are cheaper and faster. One is the reconnaisance ^{14}C dating method which has slightly larger error bars than the traditional method. However it is possible to prepare 30 corals in one day with this method. The second method is the gas ion source (GIS) method, where coral samples are reacted with H_3PO_4, and the resulting CO_2 is fed directly into the accelerator mass spectrometer (AMS) system. It is possible to measure 40 corals in 1 day with this method. However there is a much higher background with the GIS-AMS (~ 0.02) than with Reconnaissance Dating (~ 0.007).

These were run with another new development in ^{14}C dating, the Gas Ion Source (GIS) at NOSAMS in WHOI. In the GIS-AMS method, coral samples were reacted with H_3PO_4, and the resulting CO_2 is fed directly into the Accelerator Mass Spectrometer (AMS) system.

3.4 RESULTS

Figure 3.1 shows the depth and age distribution of corals collected from the New England, Corner Rise, Muir and Southern Ocean seamounts. Figure 3.1 also includes previously published U-series dated corals from the New England seamounts (Robinson, Adkins et al. 2005; Robinson, Adkins et al. 2006). There are several prominent features in the distribution of corals. One is that the coral population in the North Atlantic is in general older than the Southern Ocean coral population. There are several radiocarbon dead corals in the North Atlantic but no corals older than 45,000 ^{14}C years in the Southern Ocean. During the LGM, the coral populations in the North Atlantic predominate at 1850 m which roughly corresponds to the boundary between northern and southern source water as determined by $\delta^{13}C$ and Cd/Ca measurements (Oppo and Lehman 1993; Curry and Oppo 2005; Marchitto and Broecker 2006). Although the data are sparse, a similar boundary appears in the Southern Ocean. During the glacial time period in the North Atlantic, the bottom most extent of the coral distribution remains constant at 1850 m. Similarly in the Southern Ocean there is a nearly constant depth limit of 1650 m until 18,500 ^{14}C years, after which the population bifurcates in depth.

The coral populations both in the North Atlantic and Southern Ocean respond to rapid climate changes (Dansgaard, Johnsen et al. 1993; Blunier and Brook 2001). From sediment and ice core records we know that the YD and H1 events were both times of large reorganization of the atmospheric and ocean system. These are also times when the size and the depth range of the coral population increased in the North Atlantic (Figure 3.5). Interestingly the coral populations also expanded during the LIA in the North Atlantic (Figure 3.1, Figure 3.6), after a long period of coral growth only at the shallowest depths. In contrast to the New England seamount record, the Southern Ocean coral distribution has

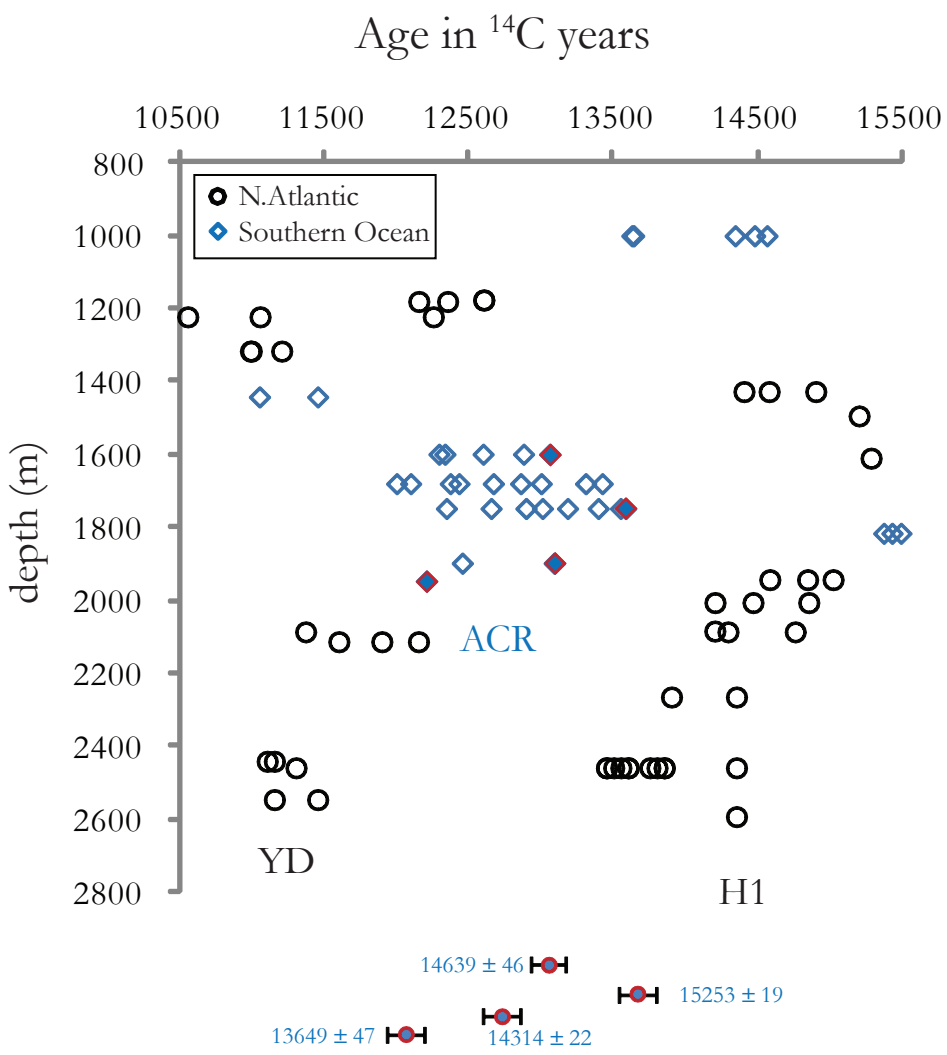

Figure 3.5: The ^{14}C age-depth distribution of deep-sea corals dated using the Reconnaissance dating method during the last deglaciation. The coral depth distribution is sharply modal during the three rapid climate changes in the deglaciation, the Younger Dryas (YD), Antarctic Cold Reversal (ACR) and Heinrich 1 (H1). Calendar ages and the associated error bars for selected ACR corals (diamonds outlined in red) are indicated at the bottom. Calendar ages for H1 and YD corals have been previously determined (36-37) and do not overlap with the ACR mode.

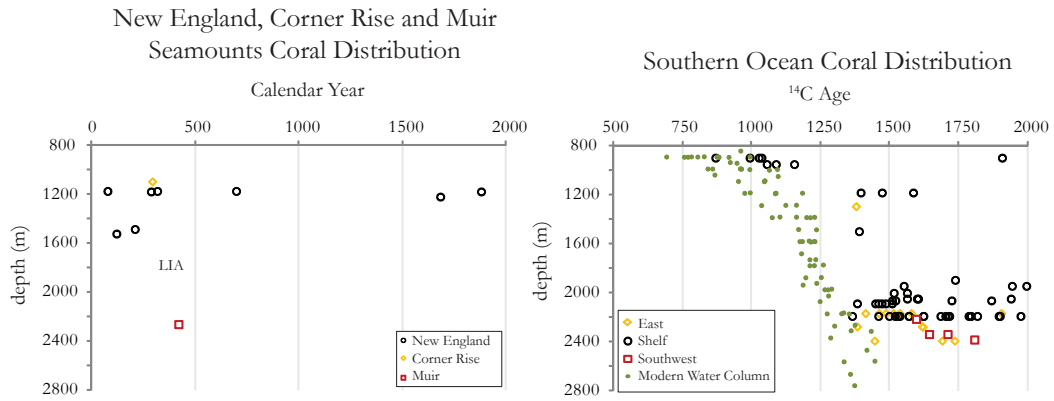

Figure 3.6: The age and depth distribution of deep-sea corals in the Late Holocene. The green diamonds represents the age of the modern water column profile. Most of the deep-sea community in the Southern Ocean is modern in radiocarbon age, while there is a mode in the deep-sea coral community in the New England sea mounts that is ~400 years old, and corresponds to the Little Ice Age (LIA).

only one deglacial mode, the Antarctic Cold Reversal (ACR). This Southern Ocean mode is different in both ^{14}C and U/Th ages (Figure 3.5, Table 3.4). As radiocarbon dates in the deep ocean, and especially in the Southern Ocean, have a large 'reservoir age', it is not possible to say with ^{14}C dates alone if the coral populations in Figure 3.2 are truly separate from one another. To check these results we selected four samples from the ACR mode in Figure 1 for U-series dating. The results are shown at the bottom of Figure 3.5. This cluster of calendar ages clearly predates that age of the start of the Younger Dryas and post-date the calendar ages of North Atlantic corals from the Heinrich Stadial interval (11). Our data show that deep ocean populations respond dramatically to local climate switches and that the populations in the North Atlantic and the Southern Ocean expanded at separate times during the last deglaciation.

In Figure 3.4 we explore the value of three different dating methods, U-series, reconnaissance ^{14}C dating and the gas ion source (GIS) method. The corals selected for analysis on the GIS-AMS were collected between 1350–1575 m of water depth. With this high frequency sampling we observe the minimum depth of the ACR to be 1575 m as corals do not appear in shallower depths. Also unlike the depth distribution of corals from the entire water column in the Southern Ocean, the depth distribution of corals at intermediate depths prefers Stage 3 relative to the Holocene. The Holocene mode is more strongly seen deeper in the water column (1800–2400 m). In the intermediate water column depths, there are two pulses in the Stage 3 mode, possibly correlated with Heinrich 3 and Heinrich 4 (Fig 3.4). These two pulses also correlate with two pulses seen in the Southern Ocean Reconnaissance data set, and perhaps with other smaller modes seen in the North Atlantic Reconnaissance data set which correspond to the other Heinrich Events (Figure 3.4).

3.5 DISCUSSION

While the overall picture of coral population dynamics is clear from Figure 3.1, we seek a more in-depth description of these results. We use the Wilcoxon rank sum test and Brown-Forsythe test to quantitatively assess the difference in medians and variances of the

different coral population shifts in depth (Table 3.3). For any single time period we bin all the coral depths and then calculate a mean and variance of this grouping. The population between 20,000 and 30,000 years in the North Atlantic is a unique distribution in mean depth compared to other North Atlantic time intervals in the Holocene and deglaciation and unique in depth variance compared to other North Atlantic time intervals during the glacial. We interpret this as a unique depth distribution for the LGM even though the age range we picked was widened to include enough corals to be statistically meaningful. In variance tests, H1 has a different value than does the YD as more corals expanded to shallower depths in the YD. The ACR distribution is also unique compared to all other times in the Southern Ocean and the YD and H1 in the North Atlantic. To further quantify our results, a targeted selection of our Southern Ocean corals was analyzed by the Gas Ion Source-AMS (GIS-AMS). Corals collected between 1350–1550 m were chosen to test the robustness of our observations of coral distributions in time, based on the reconnaissance method. The GIS allows us to analyze even more corals in a short period of time and can therefore target specific questions related to gaps in the record. As the ACR does not appear in the corals sampled from 1372 to 1500 m in the GIS results, the minimum population depth of the ACR is 1575 m (Figure 3.4). This data set also confirms the scarcity of corals during the LGM in the Southern Ocean as more corals do not appear with this higher frequency sampling.

Given these dramatic changes in coral populations in space and time, we can speculate on the factors that could affect the distributions. One possibility is a sampling bias at the field site in which the distribution of corals collected does not reflect the distribution of corals on the ocean floor. However, the coral distribution collected from the North Atlantic does not correlate with the amount of time spent looking for corals at each depth, making such a bias unlikely (Robinson, Adkins et al. 2007). Skeletal dissolution cannot explain all the diversity patterns because there are several cases where older corals survived multiple younger gaps in the population distribution at their depth. We believe that the

bottom of the ocean was randomly sampled during our dives and that our coral collection was essentially randomly sampled back on shore when we selected samples for ^{14}C dating (see Methods).

The modern distribution in the Southern Ocean has a distinctive gap between 1575–1825m that could help elucidate the factors controlling population depth preferences. It is unlikely that either a single water mass or dissolved nutrient supply is the dominant control on coral distribution because the gap does not correspond to the minimum in the salinity profile or the maximum in the phosphate or nitrate profile. Temperature is decreasing monotonically through the depth profile and is therefore not likely to be the single factor in determining coral growth in the modern. However it is possible that temperature is not low enough to be a limiting factor on coral growth at these depths and could be an important factor during other time periods. The gap does correspond to the oxygen minimum zone (OMZ) of 165 μmol/kg and the $[CO_3^{2-}]$ minimum of 110 μM in profiles from near our sampling sites (Figure 3.7). Recent work on another cosmopolitan deep-sea coral, *Lophelia pertusa*, has shown that the respiration rate of this species markedly declines at an oxygen concentration of approximately ~ 100–150 μmol/kg, depending on the growth temperature (Lawrence, Liu et al. 2006). This is a nice correspondence between lab based metabolic limits and our field based gap in the coral population. A temporary extinction of cold-water corals has also been seen from 11.4–5.9 cal kyr BP in the eastern Mediterranean (Fink, Wienberg et al. 2012). From 1400–2400 m the aragonite saturation state of the water column remains relatively constant at $\Omega \sim 0.9$, but below this depth it begins to decrease much more rapidly corresponding to the bottom-most extent of the coral distribution. So, below the oxygen minimum zone, oxygen concentrations increase and the coral populations again begin to thrive, despite low $[CO_3^{2-}]$. This suggests that the gap in coral distribution at this site is a function of declining coral respiration rate and that the bottom-most extent of the coral distribution, similar to the distribution of living *D. dianthus*, is a function of the aragonite saturation state of the water column.

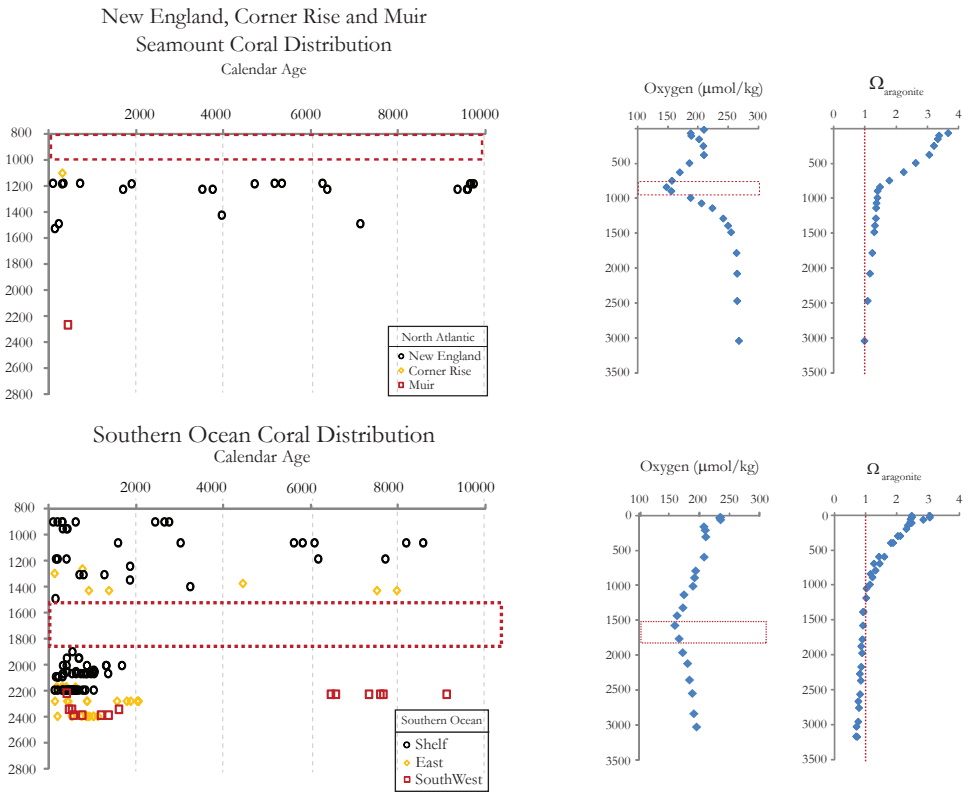

Figure 3. 7: The age-depth distributions of Holocene deep-sea corals. These corals were dated using the reconnaissance dating method (and then converted to calendar ages) and the U/Th method (19). The dashed red boxes represent gaps in the coral distribution which also correspond to the oxygen minimum zones. The dashed red lines on the $\Omega_{aragonite}$ profile represent the division between undersaturated and supersaturated water column conditions for aragonite precipitation.

Deep-sea corals are sessile filter feeders, so it is likely that surface ocean productivity is another important factor in controlling coral growth. Annual and decadal time-series studies in the modern ocean show that deep-sea biota can experience rapid changes due to variations in surface ocean productivity (Robinson and Sigman 2008; Benway, McManus et al. 2010). On longer timescales, previous work (Manighetti, McCave et al. 1995), has shown a relationship between changes in coral distributions and productivity that was attributed to changes in the location of the polar front. When all the population studies published to date are considered along with our current data set, we see a similar pattern. During the Holocene, there are abundant corals in the upper water column of the New England Seamounts, in the Rockall Trough and Porcupine Seabight regions near Iceland (Barnosky, Koch et al. 2004), and in the Sula Reef complex on the Norwegian Shelf (Marcus 1984). All of these regions are located in the subpolar gyre, or at the northern edge of the Gulf Stream and are regions of relatively high productivity. But there are few to rare occurrences of modern and Holocene deep-sea corals in the Corner Rise or the Gulf of Cadiz (Wienberg, Hebbeln et al. 2009) which are low productivity regions south of the Gulf Stream and in the subtropical gyre. In contrast, during the last glacial, atmospheric and oceanic circulation are thought to be more zonal perhaps indicating that the subpolar gyre itself was more zonally oriented. At this time there were corals in the New England and Corner Rise seamounts, as well as the Gulf of Cadiz, but none in the Rockall Trough, Porcupine Seabight or the Sula Reef complex. These latter three were north of the IRD belt and likely under sea ice with less surface productivity to fuel coral growth. In the Southern hemisphere, on the other hand, the ACR population mode does not spread across all depths as one would predict based on productivity control alone. So while surface productivity is a factor influencing coral growth in general, it cannot be the only factor in the area south of Tasmania.

This ecological dataset also has implications for our interpretation of past ocean conditions. Since the LGM, the Southern Ocean corals have increased in maximum depth. This could be due to a deepening of the aragonite saturation horizon. If the bottom-

most extent of the coral distribution during the LGM is controlled by [CO_3^{2-}] under saturation (where $\Omega < 0.9$) and not [O_2] (as there was more oxygen in the water column due to increased solubility with cooler temperatures), then the [CO_3^{2-}] at the base of the distribution during the LGM should be similar to that of the base of the modern except for temperature and pressure differences. Therefore, assuming that during the LGM, sea level is 125 m lower, the temperature is 2°C cooler (Cutler, Edwards et al. 2003), and there is a salinity increase of 3.3% (Adkins, McIntyre et al. 2002), we calculate that the [CO_3^{2-}] at 1575 m during the LGM was ~ 85 μM. This estimate for [CO_3^{2-}] during the LGM agrees with an estimate based on foraminifer dissolution rates (Sanyal, Hemming et al. 1995; Broecker 1998).

References:

Adkins, J.F., Griffin, S., Kashgarian, M., Cheng, H., Druffel, E.R.M., Boyle, E.A., Edwards, R.L., Shen, C.-C., 2002a. Radiocarbon dating of deep-sea corals. Radiocarbon 44, 567–580.

Adkins, J.F., McIntyre, K., Schrag, D.P., 2002b. The salinity, temperature, and delta O-18 of the glacial deep ocean. Science 298, 1769–1773.

Barnosky, A.D., Koch, P.L., Feranec, R.S., Wing, S.L., Shabel, A.B., 2004. Assessing the Causes of Late Pleistocene Extinctions on the Continents. Science 306, 70–75.

Benway, H.M., McManus, J.F., Oppo, D.W., Cullen, J.L., 2010. Hydrographic changes in the eastern subpolar North Atlantic during the last deglaciation. Quaternary Sci Rev 29, 3336–3345.

Blunier, T., Brook, E., 2001. Timing of millennial-scale climate change in Antarctica and Greenland during the last glacial period. Science 291, 109–112.

Boyle, E.A., Keigwin, L.D., 1982. Deep circulation of the North Atlantic over the last 200,000 years: Geochemical evidence. Science 218, 784–787.

Broecker, W.S., 1998. Paleocean Circulation during the Last Deglaciation: A Bipolar Seesaw? Paleoceanography 13, 119–121.

Burke, A., Robinson, L.F., McNichol, A.P., Jenkins, W.J., Scanlon, K.M., Gerlach, D.S., 2010. Reconnaissance dating: A new radiocarbon method applied to assessing the temporal distribution of Southern Ocean deep-sea corals. Deep Sea Research Part I: Oceanographic Research Papers 57, 1510–1520.

Cairns, S.D., 2007. Deep-water corals: An overview with special reference to diversity and distribution of deep-water scleractinian corals. B Mar Sci 81, 311–322.

Cheng, H., Adkins, J.F., Edwards, R.L., Boyle, E.A., 2000. U-Th dating of deep-sea corals. Geochimica et Cosmochimca Acta 64, 2401–2416.

Cronin, T.M., Raymo, M.E., 1997. Orbital forcing of deep-sea benthic species diversity.

Nature 385, 624–627.

Curry, W.B., Lohmann, G.P., 1985. Carbon deposition rates and deep water residence time in the equatorial Atlantic ocean throughout the last 160,000 years, in: Sundquist, E.A., Broecker, W.S. (Eds.), The Carbon Cycle and Atmospheric CO2: Natural Variations Archean to Present. Am. Geophys. Union, Geophys. Mon. 32, pp. 285–301.

Curry, W.B., Oppo, D., 2005. Glacial Water Mass Geometry and the Distribution of d13C of Total CO2 in the Western Atlantic Ocean. Paleoceanography 20, doi:10.1029/2004PA001021.

Cutler, K.B., Edwards, R.L., Taylor, F.W., Cheng, H., Adkins, J., Gallup, C.D., Cutler, P.M., Burr, G.S., Chappell, J., Bloom, A.L., 2003. Rapid sea-level fall and deep-ocean temperature change since the last interglacial. Earth Planet Sc Lett 206, 253–271.

Dansgaard, W., Johnsen, S.J., Clausen, H.B., Dahl-Jensen, D., Gundestrup, N.S., Hammer, C.U., Hvidberg, C.S., Steffensen, J.P., Sveinbjornsdottir, A.E., Jouzel, J., Bond, G., 1993. Evidence of general instability of past climate from a 250-kyr ice-core record. Nature 364, 218–220.

Eltgroth, S.F., Adkins, J.F., Robinson, L., Southon, J., Kashgarian, M., 2006. A deep-sea coral record of North Atlantic radiocarbon through the Younger Dryas: Evidence for Intermediate/Deep water reorganization. Paleoceanography.

Fink, H.G., Wienberg, C., Hebbeln, D., McGregor, H.V., Schmiedl, G., Taviani, M., Freiwald, A., 2012. Oxygen control on Holocene cold-water coral development in the eastern Mediterranean Sea. Deep Sea Research Part I: Oceanographic Research Papers 62, 89-96.

Lawrence, K.T., Liu, Z., Herbert, T.D., 2006. Evolution of the Eastern Tropical Pacific Through Plio-Pleistocene Glaciation. Science 312, 79–83.

Manighetti, B., McCave, I.N., Maslin, M., Shackleton, N.J., 1995. Chronology for Climate Change: Developing Age Models for the Biogeochemical Ocean Flux Study Cores. Paleoceanography 10, 513–525.

Marchitto, T.M., Broecker, W., 2006. Deep water mass geometry in the glacial Atlantic Ocean: A review of constraints from the paleonutrient proxy Cd/Ca. Geochem Geophy Geosy 7, doi:10.1029/2006GC001323.

Marcus, L.a.B., R, 1984. The significance of Radiocarbon Dates for Rancho La Brea, in: Martin, P.a.K., R (Ed.), Quaternary Extinctions. University of Arizona Press, Tucson, Arizona.

Oppo, D., Horowitz, M., 2000. Glacial deep water geometry: South Atlantic benthic foraminiferal Cd/Ca and delta C-13 evidence. Paleoceanography 15, 147–160.

Oppo, D.W., Lehman, S.J., 1993. Mid-depth circulation of the subpolar North Atlantic during the last glacial maximum. Science 259, 1148–1152.

Raymo, M.E., Ruddiman, W.F., Shackleton, N.J., Oppo, D.W., 1990. Evolution of Atlantic-Pacific C13 gradients over the last 2.5 m.y. Earth Planet Sc Lett 97, 353–368.

Robinson, L., Adkins, J.F., Fernandez, D.P., Burnett, D.S., Wang, S.-L., Gagnon, A.C., Krakauer, N., 2006. Primary U-distribution in scleractinian corals and its implications for U-series dating. Geochem Geophy Geosy 7, doi:10.1029/2005GC001138.

Robinson, L., Adkins, J.F., Keigwin, L.D., Southon, J., Fernandez, D.P., Wang, S.-L., Scheirer, D.S., 2005a. Radiocarbon variability in the Western North Atlantic during the last deglaciation. Science 310, 1469–1473.

Robinson, L.F., Adkins, J.F., Keigwin, L.D., Southon, J., Fernandez, D.P., Wang, S.L., Scheirer, D.S., 2005b. Radiocarbon variability in the western North Atlantic during the last deglaciation. Science 310, 1469–1473.

Robinson, L.F., Adkins, J.F., Scheirer, D., Fernandez, D.P., Gagnon, A.C., Waller, R., 2007. Deep-sea scleractinian coral age and depth distributions in the NW Atlantic for the last 225 thousand years. B Mar Sci 81, 371–391.

Robinson, R.S., Sigman, D.M., 2008. Nitrogen isotopic evidence for a poleward decrease in surface nitrate within the ice age Antarctic. Quaternary Sci Rev 27, 1076–1090.

Sanyal, A., Hemming, N.G., Hanson, G.N., Broecker, W.S., 1995. Evidence for a higher pH in the glacial ocean from boron isotopes in foraminifera. Nature 373, 234–236.

Streeter, S.S., Shackleton, N.J., 1979. Paleocirculation of the deep North Atlantic: 150,000-year record of benthic foraminifera and oxygen-18. Science 203, 168–171.

Thiagarajan, N.G., D. S.; Roberts, M.; McNichol, A. P.; Thresher, R.; Adkins, J. F., 2009. Radiocarbon Age Variability of Deep Sea Corals from the North Atlantic and the Southern Ocean, American Geophysical Union, San Francisco.

Wienberg, C., Hebbeln, D., Fink, H.G., Mienis, F., Dorschel, B., Vertino, A., Correa, M.L., Freiwald, A., 2009. Scleractinian cold-water corals in the Gulf of Cádiz—First clues about their spatial and temporal distribution. Deep Sea Research Part I: Oceanographic Research Papers 56, 1873–1893.

Xu, X., Trumbore, S.E., Zheng, S., Southon, J.R., McDuffee, K.E., Luttgen, M., Liu, J.C., 2007. Modifying a sealed tube zinc reduction method for preparation of AMS graphite targets: Reducing background and attaining high precision. Nuclear Instruments and Methods in Physics Research Section B: Beam Interactions with Materials and Atoms 259, 320–329.

Table 3.1-Radiocarbon and Calendar ages for North Atlantic deep-sea corals with their unique sample name, seamount, and depth

Name	Depth	Lab Code	Seamount	Region	F Modern	Fm Error	Libby Age	Age Error	Calendar Age
RBDASS05-H05_0818-1926-103-001-1098	1098	UBA06	VERRILL	Corner Rise	0.9003	0.0044	845	40	291
RBDASS05-H05_0818-1450-101-004-1316	1316	UBA04	VERRILL	Corner Rise	0.2485	0.0017	11200	55	11902
RBDASS05-H07-0821-0513-112-007-1929	1929	NTWH2-A01	GOODE	Corner Rise	0.0226	0.0017	30441	614	33940
RBDASS05-H07-0821-0513-112-013-1929	1929	NTWH2-A03	GOODE	Corner Rise	0.0203	0.0017	31325	689	34931
RBDASS05-H07-0821-0513-112-008-1929	1929	NTWH2-A10	GOODE	Corner Rise	0.0224	0.0017	30503	618	33994
RBDASS05-H09-0823-0225-216-022-1610	1610	NTWH2-B10	KUK	Corner Rise	0.1492	0.0017	15283	89	17371
RBDASS05-h09-0822-1800-201-001-1840	1840	NTWH2-B11	KUK	Corner Rise	0.0239	0.0017	29997	578	33534
RBDASS05-h09-0822-1800-201-002-1840	1840	NTWH2-B13	KUK	Corner Rise	0.1445	0.0017	15541	92	17697
RBDASS05-h09-0823-0349-217-012-1494	1494	NTWH2-B15	KUK	Corner Rise	0.0741	0.0017	20906	183	23783
RBDASS05-h09-0823-0349-217-007-1494	1494	NTWH2-B19	KUK	Corner Rise	0.1507	0.0017	15200	89	17281
RBDASS05-h09-0823-0349-217-009-1494	1494	ntwh2-b20	KUK	Corner Rise	0.0332	0.0015	27346	351	30945
RBDASS05-h09-0823-0225-216-006-1610	1610	ntwh2-b22	KUK	Corner Rise	0.0797	0.0014	20316	142	23013
RBDASS05-h09-0823-0225-216-002-1610	1610	ntwh2-b23-2	KUK	Corner Rise	0.0278	0.0014	28770	414	32031
RBDASS05-h09-0822-1800-201-003-1840	1840	NTWH2-B25	KUK	Corner Rise	0.1429	0.0018	15628	101	17796
RBDASS05-H03-0815-0156-304-001-1583	1583	NTWH2-A02	LYMAN	Corner Rise	0.0701	0.0017	21349	194	24277
RBDASS05-H03-0815-0156-304-005-1583	1583	NTWH2-A04	LYMAN	Corner Rise	0.0507	0.0017	23953	272	27718
RBDASS05-H03-0814-2151-301-003-1634	1634	NTWH2-A07	LYMAN	Corner Rise	0.0314	0.0017	27806	439	31226
RBDASS05-H03-0815-1004-314-3-003-1427	1427	NTWH2-A08	LYMAN	Corner Rise	0.0041	0.0017	44216	3450	46317
RBDASS05-h03-0815-0156-304-007-1583	1583	NTWH2-B24	LYMAN	Corner Rise	0.0799	0.0018	20302	184	22997
RBDASS05-H03-0815-1004-314-3-001-1427	1427	NTWH2-H48	LYMAN	Corner Rise	0.1565	0.0018	14899	90	16974
RBDASS05-H03-0815-1004-314-3-002-1427	1427	NTWH2-H49	LYMAN	Corner Rise	0.1629	0.0018	14576	88	16734
RBDASS05-H03-0815-1004-314-3-002-1427	1427	NTWH2-h49-2	LYMAN	Corner Rise	0.1665	0.0026	14402	125	16492
RBDASS05-H03-0814-2151-301-007-1634	1634	NTWH2-H50	LYMAN	Corner Rise	0.0253	0.0014	29534	454	32914
RBDASS05-H03-0814-2151-301-011-1634	1634	NTWH2-H51	LYMAN	Corner Rise	0.0251	0.0014	29600	457	33013
ALV-4162-1916-008-033-1943	1943	NTWH2-B08	PICKETT	Corner Rise	0.1542	0.0018	15019	91	17074
ALV-4162-1628-003-014-2006	2006	NTWH2-B09	PICKETT	Corner Rise	0.1574	0.0017	14851	86	16939
ALV-4162-1916-008-009-1943	1943	NTWH2-B12	PICKETT	Corner Rise	0.1576	0.0018	14843	94	16935
ALV-4162-1457-001-003-2086	2086	NTWH2-B14	PICKETT	Corner Rise	0.2429	0.0018	11366	60	12236
ALV-4162-1457-001-004-2086	2086	NTWH2-B16	PICKETT	Corner Rise	0.1688	0.0016	14291	78	16315
ALV-4162-1628-003-034-2006	2006	NTWH2-B17	PICKETT	Corner Rise	0.1652	0.0016	14465	80	16634
ALV-4162-1628-003-024-2006	2006	NTWH2-B18	PICKETT	Corner Rise	0.1707	0.0019	14201	89	16092
ALV-4162-1916-008-030-1943	1943	NTWH2-B21	PICKETT	Corner Rise	0.1628	0.0020	14581	99	16733
ALV-4162-1457-001-002-2086	2086	NTWH2-B26	PICKETT	Corner Rise	0.1593	0.0018	14757	90	16876
RBDASS05-H06-0819-1631-210-5-012-1640	1640	NTWH2-A05	VERRILL	Corner Rise	0.0696	0.0017	21406	195	24349
RBDASS05-H06-0819-1019-205-001-1950	1950	NTWH2-A06	VERRILL	Corner Rise	0.0067	0.0018	40251	2168	43407
RBDASS05-H05-0818-1450-101-003-1316	1316	NTWH2-A09	VERRILL	Corner Rise	0.2546	0.0016	10989	51	10760
RBDASS05-H06-0819-0534-201-5-001-2113	2113	NTWH2-B01	VERRILL	Corner Rise	0.2204	0.0016	12148	60	13028
RBDASS05-H06-0819-0534-201-5-007-2113	2113	NTWH2-B02	VERRILL	Corner Rise	0.2275	0.0019	11894	65	12768
RBDASS05-H06-0819-1019-205-017-1950	1950	NTWH2-B03	VERRILL	Corner Rise	0.0068	0.0017	40060	2041	43271
RBDASS05-H06-0819-0534-201-5-004-2113	2113	NTWH2-B04-2	VERRILL	Corner Rise	0.2361	0.0016	11596	56	12553
RBDASS05-H06-0819-1019-205-012-1950	1950	NTWH2-B05	VERRILL	Corner Rise	0.0067	0.0017	40189	2078	43367
RBDASS05-H06-0819-1631-210-5-020-1640	1640	NTWH2-B06	VERRILL	Corner Rise	0.0735	0.0017	20974	187	23865
RBDASS05-H06-0819-1631-210-5-019-1640	1640	NTWH2-B07	VERRILL	Corner Rise	0.0799	0.0017	20303	170	22998
RBDASS05-H05-0818-1450-101-001-1316	1316	UBA01	VERRILL	Corner Rise	0.2548	0.0014	10984	45	10742
ALV-3887-1436-003-020	2441	UBA11	Muir	Muir	0.2510	0.0016	11100	55	11698
ALV-3887-1436-003-017	2441	UBA08	Muir	Muir	0.2499	0.0018	11150	60	11816
ALV-3887-1324-002-001	2546	UBB02	Muir	Muir	0.2503	0.0018	11150	55	11820
ALV-3887-1324-002-006	2546	UBA18	Muir	Muir	0.2400	0.0019	11450	60	12356
ALV-3887-1652-005-B8	2265	UAN08	Muir	Muir	0.1773	0.0020	13900	90	15444
ALV-3884-1638-004-154	2084	UAK17	Muir	Muir	0.1712	0.0018	14200	85	16093
ALV-3887-1652-005-B2	2265	UAN07	Muir	Muir	0.1681	0.0019	14350	90	16447
ALV-3885-1239-001-010	2027	UAH19	Muir	Muir	0.1150	0.0018	17350	130	19506
ALV-3885-1452-004-027	1878	UAN02	Muir	Muir	0.0156	0.0020	33400	1000	37096
ALV-3885-1452-004-028	1878	UAN05	Muir	Muir	0.0088	0.0020	38100	1800	41686
ALV-3885-1452-004-025	1878	UAN03	Muir	Muir	0.0080	0.0020	38800	2000	42258
ALV-3885-1452-004-026	1878	UAN04	Muir	Muir	0.0072	0.0020	39600	2200	42886
ALV-3889-1353-003-002	1714	UAM02	Muir	Muir	0.0027	0.0020	60000	6000	60000
ALV-3887-1436-003-021	2441	UBA12	Muir	Muir	0.0023	0.0020	60000	6900	60000
ALV-3887-1436-003-022	2441	UBA13	Muir	Muir	0.0018	0.0020	60000	8800	60000
ALV-3887-1436-003-002	2441	UBA19	Muir	Muir	0.0032	0.0020	60000	5000	60000
ALV-3889-1326-002-001	1723	UAM03	Muir	Muir	Indistinguishable from background	0.0000	60000		60000
ALV-3891-1646-004-005	1180	UAJ10	Gregg	New Eng	0.9019	0.0024	830	20	285
ALV-3891-1459-003-012	1176	UAM14	Gregg	New Eng	0.8434	0.0025	1370	25	696
ALV-3891-1758-006-004	1222	UAM13	Gregg	New Eng	0.7447	0.0027	2370	30	1682
ALV-3891-1646-004-B1	1180	UBA02	Gregg	New Eng	0.7295	0.0027	2530	30	1879
ALV-3891-1758-006-011	1222	UBB07	Gregg	New Eng	0.6179	0.0016	3870	20	3499
ALV-3891-1758-006-012	1222	UBB08	Gregg	New Eng	0.6032	0.0022	4060	30	3734
ALV-3891-1459-003-008	1176	UAM19	Gregg	New Eng	0.5277	0.0016	5130	25	5154
ALV-3891-1459-003-008	1176	UAM19	Gregg	New Eng	0.5234	0.0015	5200	25	5321
ALV-3891-1758-006-002	1222	UAM18	Gregg	New Eng	0.4625	0.0016	6190	25	6361
ALV-3891-1758-006-010	1222	UBB06	Gregg	New Eng	0.3285	0.0030	8940	75	9347
ALV-3891-1758-006-010	1222	UBB06	Gregg	New Eng	0.3173	0.0018	9220	45	9582
ALV-3891-1646-004-002	1180	UAO05	Gregg	New Eng	0.3150	0.0020	9280	50	9633
ALV-3891-1646-004-006	1180	UAO04	Gregg	New Eng	0.3138	0.0016	9310	40	9656

ALV-3891-1646-004-002	1180	UAO05	Gregg	New Eng	0.3128	0.0017	9340	45	9717
ALV-3891-1758-006-009	1222	UBB05	Gregg	New Eng	0.2838	0.0018	10100	50	9562
ALV-3891-1725-005-B2	1222	UBB10	Gregg	New Eng	0.2695	0.0017	10550	50	10219
ALV-3891-1758-006-001	1222	UAM20	Gregg	New Eng	0.2529	0.0017	11050	55	10915
RBDASS05-H15_0831-2045-605-053-2459	2459	UCA06	Kelvin	New Eng	0.2448	0.0018	11300	60	12103
ALV-3891-1646-004-001	1180	UAO01	Gregg	New Eng	0.2201	0.0017	12150	65	13030
ALV-3891-1725-005-006	1222	UAN10	Gregg	New Eng	0.2177	0.0018	12250	65	13158
ALV-3891-1646-004-007	1180	UAN11	Gregg	New Eng	0.2145	0.0021	12350	75	13231
ALV-3891-1459-003-018	1176	UAN06	Gregg	New Eng	0.2090	0.0017	12600	65	13440
ALV-3891-1459-003-018	1176	UAN06	Gregg	New Eng	0.2090	0.0017	12600	65	13440
RBDASS05-H15_0831-2045-605-003-2459	2459	UCA03	Kelvin	New Eng	0.1870	0.0017	13450	75	14554
RBDASS05-H15_0831-2045-605-035-2459	2459	UCB17	Kelvin	New Eng	0.1876	0.0017	13450	75	14554
RBDASS05-H15_0831-2045-605-034-2459	2459	UCB16	Kelvin	New Eng	0.1866	0.0018	13500	75	14646
RBDASS05-H15_0831-2045-605-036-2459	2459	UCB18	Kelvin	New Eng	0.1849	0.0017	13550	75	14736
RBDASS05-H15_0831-2045-605-013-2459	2459	UBB20	Kelvin	New Eng	0.1837	0.0018	13600	80	14837
RBDASS05-H15_0831-2045-605-033-2459	2459	UCB15	Kelvin	New Eng	0.1835	0.0019	13600	85	14830
RBDASS05-H15_0831-2045-605-008-2459	2459	UBB18	Kelvin	New Eng	0.1806	0.0017	13750	75	15130
RBDASS05-H15_0831-2045-605-037-2459	2459	UCB19	Kelvin	New Eng	0.1794	0.0017	13800	80	15230
RBDASS05-H15_0831-2045-605-001-2459	2459	UCA01	Kelvin	New Eng	0.1787	0.0019	13850	85	15351
RBDASS05-H15_0831-2045-605-007-2459	2459	UCA10	Kelvin	New Eng	0.1778	0.0019	13850	85	15351
RBDASS05-H15_0831-1616-601_3-003-2593	2593	UBB17	Kelvin	New Eng	0.1675	0.0019	14350	90	16447
RBDASS05-H15_0831-2045-605-020-2459	2459	UCA05	Kelvin	New Eng	0.1676	0.0018	14350	85	16454
ALV-3891-1725-005-009	1222	UAI08	Gregg	New Eng	0.0112	0.0020	36100	1400	39925
ALV-3890-1718-006-004	1421	UAL01	Manning	New Eng	0.0026	0.0020	60000	6200	39600

Table 3.2-Radiocarbon and Calendar ages for Southern Ocean deep-sea corals with their unique sample name, seamount, and depth

Name	Lab Code	Seamount	Region	Depth	F Modern	Fm Error	Libby Age	Age Error	Calendar Age
TN228-J2-387-1225-1253-11-1898-001	ESA01	S.HILLS	SHELF	1898	0.19605	0.00164	13089	67.1	13086
TN228-J2-387-1225-1253-11-1898-002	ESA02	S.HILLS	SHELF	1898	0.21222	0.00163	12452	61.6	12497
TN228-J2-387-1225-1253-11-1898-003	ESA03	S.HILLS	SHELF	1898	0.80539	0.00169	1739	16.9	521
TN228-J2-387-1224-2355-1-2051-001	ESC02	S.HILLS	SHELF	2051	0.78538	0.00239	1941	24.4	602
TN228-J2-387-1224-2355-1-2051-002	ESC03	S.HILLS	SHELF	2051	0.82301	0.00336	1565	32.8	387
TN228-J2-387-1224-2355-1-2051-003	ESC04	S.HILLS	SHELF	2051	0.81887	0.00379	1605	37.2	399
TN228-J2-395-0113-0902-01-2193-001	ESC07	S.HILLS	SHELF	2193	0.82967	0.00183	1500	17.7	291
TN228-J2-395-0113-0902-01-2193-002	ESC08	S.HILLS	SHELF	2193	0.78948	0.00167	1899	17.0	589
TN228-J2-395-0113-0902-01-2193-003	ESC09	S.HILLS	SHELF	2193	0.76736	0.00164	2127	17.1	763
TN228-J2-395-0113-0902-01-2193-003	ESC09	S.HILLS	SHELF	2193	0.76518	0.00293	2150	30.7	818
TN228-J2-395-0113-0902-01-2193-004	ESD01	S.HILLS	SHELF	2193	0.80801	0.00236	1713	23.4	513
TN228-J2-395-0113-0902-01-2193-006	ESD02	S.HILLS	SHELF	2193	0.82753	0.00221	1521	21.4	306
TN228-J2-395-0113-0902-01-2193-006	ESD02	S.HILLS	SHELF	2193	0.82640	0.00175	1532	17.0	308
TN228-J2-395-0113-1830-5-1947-002	ESD03	S.HILLS	SHELF	1947	0.77987	0.00182	1997	18.7	674
TN228-J2-395-0113-1830-5-1947-003	ESD04	S.HILLS	SHELF	1947	0.21889	0.00164	12204	60.2	12112
TN228-J2-395-0113-1830-5-1947-004	ESD05	S.HILLS	SHELF	1947	0.82418	0.00172	1553	16.8	394
TN228-J2-395-0113-1830-5-1947-005	ESD07	S.HILLS	SHELF	1947	0.78491	0.00167	1945	17.1	664
TN228-J2-387-1225-0147-02-2066-02	ESD08	S.HILLS	SHELF	2066	0.71311	0.00157	2716	17.7	1340
TN228-J2-387-1225-0147-02-2066-03	ESD09	S.HILLS	SHELF	2066	0.77207	0.00182	2078	19.0	714
TN228-J2-387-1225-0147-02-2066-04	ESD10	S.HILLS	SHELF	2066	0.74696	0.00196	2344	21.1	947
TN228-J2-387-1225-0147-02-2066-05	ESD11	S.HILLS	SHELF	2066	0.76190	0.00183	2184	19.3	855
TN228-J2-387-1225-0147-02-2066-06	ESD12	S.HILLS	SHELF	2066	0.82725	0.00261	1523	25.4	314
TN228-J2-387-1226-1148-20-1680-001	ESE01	S.HILLS	SHELF	1680	0.21442	0.00162	12369	60.6	12407
TN228-J2-387-1226-1148-20-1680-002	ESE02	S.HILLS	SHELF	1680	0.18812	0.00165	13421	70.4	13369
TN228-J2-387-1226-1148-20-1680-003	ESE03	S.HILLS	SHELF	1680	0.19082	0.00166	13306	69.8	13276
TN228-J2-387-1226-1148-20-1680-004	ESE04	S.HILLS	SHELF	1680	0.21284	0.00168	12429	63.5	12476
TN228-J2-392-0110-1409-08-2225-03	ESE06	FINGER	SOUTHWEST	2225	0.36652	0.00148	8063	32.4	7578
TN228-J2-384-1218-0950-02-0952-03	ESF05	S.HILLS	SHELF	952	0.87666	0.00183	1057	16.8	300
TN228-J2-384-1218-0950-02-0952-01	ESF06	S.HILLS	SHELF	952	0.00959	0.00188	37332	1573.4	40179
TN228-J2-384-1218-0950-02-0952-04	ESF07	S.HILLS	SHELF	952	0.86596	0.00238	1156	22.1	407
TN228-J2-384-1218-0950-02-0952-06	ESG02	S.HILLS	SHELF	952	0.87315	0.00262	1090	24.1	388
TN228-J2-386-1223-1345-011-0899-001	ESG03	S.HILLS	SHELF	899	0.59844	0.00195	4124	26.1	2737
TN228-J2-386-1223-1345-011-0899-002	ESH01	S.HILLS	SHELF	899	0.62055	0.00254	3833	32.9	2629
TN228-J2-386-1223-1345-011-0899-004	ESH03	S.HILLS	SHELF	899	0.78853	0.00222	1909	22.7	596
TN228-J2-386-1223-1345-011-0899-008	ESH04	S.HILLS	SHELF	899	0.62354	0.00235	3794	30.3	2417
TN228-J2-386-1223-1345-011-0899-009	ESH05	S.HILLS	SHELF	899	0.88352	0.00302	995	27.5	179
TN228-J2-386-1223-0739-07-0958-001	ESH06	S.HILLS	SHELF	958	0.03656	0.00150	26580	329.6	29528
TN228-J2-386-1223-0739-07-0958-003	ESH07	S.HILLS	SHELF	958	0.03210	0.00193	27625	482.1	30485
TN228-J2-386-1223-0739-07-0958-003	ESH07	S.HILLS	SHELF	958	0.03139	0.00146	27804	374.0	30660
TN228-J2-386-1223-0739-07-0958-005	ESH08	S.HILLS	SHELF	958	0.02436	0.00188	29841	618.5	32310
TN228-J2-386-1223-0739-07-0958-005	ESH08-2	S.HILLS	SHELF	958	0.01063	0.00144	36506	1088.3	39550
TN228-J2-386-1223-0739-07-0958-008	ESI01	S.HILLS	SHELF	958	0.01237	0.00145	35287	940.4	38130
TN228-J2-386-1223-0739-07-0958-009	ESI02	S.HILLS	SHELF	958	0.02666	0.00143	29116	432.4	31506
TN228-J2-386-1223-0515-04-1000-001	ESI03	S.HILLS	SHELF	1000	0.16319	0.00213	14562	105.0	14945
TN228-J2-386-1223-0515-04-1000-002	ESI04	S.HILLS	SHELF	1000	0.16773	0.00169	14342	81.1	14541
TN228-J2-386-1223-0515-04-1000-003	ESJ01	S.HILLS	SHELF	1000	0.18334	0.00140	13627	61.5	13576
TN228-J2-386-1223-0515-04-1000-007	ESJ02	S.HILLS	SHELF	1000	0.16495	0.00174	14476	84.5	14779
TN228-J2-386-1223-0515-04-1000-008	ESJ03	S.HILLS	SHELF	1000	0.18308	0.00156	13639	68.5	13588
TN228-J2-390-0104-0815-968-002	ESJ04	CASCADE	EAST	968	0.02155	0.00190	30824	709.0	33402
TN228-J2-390-0104-0815-968-006	ESJ05	CASCADE	EAST	968	0.02434	0.00188	29846	620.2	32315
TN228-J2-390-0104-0815-968-007	ESJ06	CASCADE	EAST	968	0.01304	0.00188	34860	1160.1	37719
TN228-J2-390-0104-0815-968-008	ESJ07	CASCADE	EAST	968	0.01922	0.00145	31746	606.8	34351
TN228-J2-390-0104-0815-968-009	ESJ08	CASCADE	EAST	968	0.01349	0.00143	34586	853.2	37404
TN228-J2-389-0101-0330-01-1428-001	ESJ09	EAST OF ST. HELENS	EAST	1428	0.69753	0.00228	2894	26.3	1360
TN228-J2-389-0101-0330-01-1428-002	ESJ10	EAST OF ST. HELENS	EAST	1428	0.75726	0.00249	2234	26.4	898
TN228-J2-389-0101-0330-01-1428-007	ESK01	EAST OF ST. HELENS	EAST	1428	0.37144	0.00160	7956	34.6	7501
TN228-J2-389-0101-0330-01-1428-010	ESK02	EAST OF ST. HELENS	EAST	1428	0.34257	0.00163	8605	38.1	7957
TN228-J2-395-0114-0057-09-1500-004	ESK03	S.HILLS	SHELF	1500	0.03220	0.00191	27601	476.8	30467
TN228-J2-395-0114-0057-09-1500-004	ESK03-2	S.HILLS	SHELF	1500	0.03578	0.00191	26753	428.5	29720
TN228-J2-395-0114-0057-09-1500-05	ESK04	S.HILLS	SHELF	1500	0.02136	0.00143	30896	538.2	33553
TN228-J2-395-0114-0057-09-1500-07	ESK05	S.HILLS	SHELF	1500	0.00226	0.00144	48939	5120.4	48684
TN228-J2-395-0114-0057-09-1500-09	ESK06	S.HILLS	SHELF	1500	0.01780	0.00143	32360	645.9	35085
TN228-J2-387-1225-0318-3-2040-001	ESK07	S.HILLS	SHELF	2040	0.74464	0.00225	2369	24.3	1010
TN228-J2-383-1217-1611-07-1397-001	ESL01-2	S.HILLS	SHELF	1397	0.02965	0.00187	28263	507.1	30914
TN228-J2-383-1217-1611-07-1397-003	ESL02	S.HILLS	SHELF	1397	0.52294	0.00204	5208	31.4	3222
TN228-J2-395-0114-0555-17-1345-005	ESM01	S.HILLS	SHELF	1345	0.02548	0.00143	29479	450.7	31869
TN228-J2-395-0114-0555-17-1345-009	ESM02	S.HILLS	SHELF	1345	0.09707	0.00145	18736	120.0	20001
TN228-J2-395-0114-0555-17-1345-010	ESM03	S.HILLS	SHELF	1345	0.09542	0.00141	18873	118.6	20155
TN228-J2-385-1221-0558-05-1060-001	NTWH2-C01	S.HILLS	SHELF	1060	0.69383	0.00203	2936	23.5	1567
TN228-J2-385-1221-0558-05-1060-002	NTWH2-C02	S.HILLS	SHELF	1060	0.58837	0.00218	4261	29.7	3000
TN228-J2-385-1221-0558-05-1060-003	NTWH2-C03	S.HILLS	SHELF	1060	0.32413	0.00144	9050	35.7	8560

TN228-J2-385-1221-0558-05-1060-004	NTWH2-C04	S.HILLS	SHELF	1060	0.32504	0.00141	9028	34.9	8171
TN228-J2-385-1221-0558-05-1060-005	NTWH2-C05	S.HILLS	SHELF	1060	0.43908	0.00142	6612	25.9	6070
TN228-J2-385-1221-0229-04-1123-001	NTWH2-C06	S.HILLS	SHELF	1123	0.07828	0.00140	20464	143.6	22150
TN228-J2-385-1221-0229-04-1123-002	NTWH2-C07	S.HILLS	SHELF	1123	0.00566	0.00144	41566	2049.2	43725
TN228-J2-385-1221-0229-04-1123-003	NTWH2-C08	S.HILLS	SHELF	1123	0.00355	0.00144	45306	3251.0	46502
TN228-J2-385-1221-0229-04-1123-004	NTWH2-C09	S.HILLS	SHELF	1123	0.01081	0.00148	36367	1096.1	39404
TN228-J2-385-1221-0229-04-1123-005	NTWH2-C10	S.HILLS	SHELF	1123	0.00568	0.00174	41530	2451.9	43692
TN228-J2-385-1221-0229-04-1123-006	NTWH2-C11	S.HILLS	SHELF	1123	0.01215	0.00146	35430	968.4	38293
TN228-J2-385-1221-0229-04-1123-007	NTWH2-C12	S.HILLS	SHELF	1123	0.00730	0.00145	39518	1590.8	42196
TN228-J2-385-1221-0229-04-1123-008	NTWH2-C13	S.HILLS	SHELF	1123	0.00595	0.00144	41166	1945.4	43434
TN228-J2-385-1221-0229-04-1123-009	NTWH2-C14	S.HILLS	SHELF	1123	0.00834	0.00144	38456	1385.2	41304
TN228-J2-385-1221-0229-04-1123-010	NTWH2-C15	S.HILLS	SHELF	1123	0.00459	0.00144	43249	2517.6	45106
TN228-J2-385-1221-026-02-1184-001	NTWH2-C16	S.HILLS	SHELF	1184	0.42290	0.00167	6913	31.7	6154
TN228-J2-385-1221-026-02-1184-002	NTWH2-C17	S.HILLS	SHELF	1184	0.84033	0.00220	1397	21.1	144
TN228-J2-385-1221-026-02-1184-003	NTWH2-C18	S.HILLS	SHELF	1184	0.82068	0.00225	1587	22.1	386
TN228-J2-385-1221-026-02-1184-004	NTWH2-C19	S.HILLS	SHELF	1184	0.83240	0.00256	1474	24.7	182
TN228-J2-385-1221-026-02-1184-005	NTWH2-C20	S.HILLS	SHELF	1184	0.35250	0.00166	8376	37.9	7693
TN228-J2-385-1220-2149-01-1240-001	NTWH2-C21	S.HILLS	SHELF	1240	0.11839	0.00176	17141	119.4	18501
TN228-J2-385-1220-2149-01-1240-002	NTWH2-C22	S.HILLS	SHELF	1240	0.01351	0.00144	34579	856.4	37396
TN228-J2-385-1220-2149-01-1240-003	NTWH2-C23	S.HILLS	SHELF	1240	0.67460	0.00220	3162	26.2	1843
TN228-J2-385-1220-2149-01-1240-004	NTWH2-C24	S.HILLS	SHELF	1240	0.01050	0.00145	36605	1111.2	39642
TN228-J2-382-1216-1930-16-1305-001	NTWH2-C25	S.HILLS	SHELF	1305	0.72273	0.00213	2608	23.6	1254
TN228-J2-382-1216-1930-16-1305-002	NTWH2-C26	S.HILLS	SHELF	1305	0.77401	0.00233	2058	24.2	683
TN228-J2-382-1216-1930-16-1305-002	NTWH2-C26-2	S.HILLS	SHELF	1305	0.76735	0.00190	2127	19.9	776
TN228-J2-383-1217-1800-09-1346-001	NTWH2-C27	S.HILLS	SHELF	1346	0.67634	0.00218	3141	25.9	1840
TN228-J2-383-1217-1800-09-1346-002	NTWH2-C28	S.HILLS	SHELF	1346	0.01114	0.00144	36126	1037.8	39150
TN228-J2-382-1216-1820-14-1372-001	NTWH2-C29	S.HILLS	SHELF	1372	0.03334	0.00173	27321	416.2	30217
TN228-J2-382-1216-1820-14-1372-002	NTWH2-C30	S.HILLS	SHELF	1372	0.02180	0.00145	30734	536.2	33346
TN228-J2-382-1216-1820-14-1372-003	NTWH2-C31	S.HILLS	SHELF	1372	0.00687	0.00144	40011	1682.9	42584
TN228-J2-382-1216-1619-11-1433-001	NTWH2-C32	S.HILLS	SHELF	1433	0.00360	0.00176	45192	3925.4	46167
TN228-J2-382-1216-1619-11-1433-003	NTWH2-C34	S.HILLS	SHELF	1433	0.00235	0.00144	48617	4919.7	48362
TN228-J2-383-1217-1320-05-1460-001	NTWH2-C35	S.HILLS	SHELF	1460	0.00794	0.00174	38850	1756.2	41560
TN228-J2-383-1217-1320-05-1460-002	NTWH2-C36	S.HILLS	SHELF	1460	0.00862	0.00144	38188	1338.8	41068
TN228-J2-383-1217-1320-05-1460-003	NTWH2-C37	S.HILLS	SHELF	1460	0.01745	0.00145	32520	668.3	35267
TN228-J2-383-1217-1024-04-1500-001	NTWH2-D01-2	S.HILLS	SHELF	1500	0.84102	0.00303	1391	28.9	133
TN228-J2-383-1217-0725-01-1575-001	NTWH2-D02	S.HILLS	SHELF	1575	0.06177	0.00170	22366	221.2	24429
TN228-J2-383-1217-0725-01-1575-002	NTWH2-D03	S.HILLS	SHELF	1575	0.04238	0.00142	25393	268.6	28279
TN228-J2-383-1217-0725-01-1575-003	NTWH2-D04	S.HILLS	SHELF	1575	0.02923	0.00142	28376	390.9	31020
TN228-J2-383-1217-0725-01-1575-004	NTWH2-D05	S.HILLS	SHELF	1575	0.02197	0.00147	30669	536.9	33256
TN228-J2-383-1217-0725-01-1575-005	NTWH2-D06	S.HILLS	SHELF	1575	0.01326	0.00144	34729	872.6	37554
TN228-J2-383-1217-0725-01-1575-006	NTWH2-D07	S.HILLS	SHELF	1575	0.13654	0.00138	15995	81.1	17144
TN228-J2-387-1226-1635-23-1599-001	NTWH2-D08	S.HILLS	SHELF	1599	0.20130	0.00167	12876	66.6	12846
TN228-J2-387-1226-1635-23-1599-002	NTWH2-D09	S.HILLS	SHELF	1599	0.20847	0.00141	12596	54.2	12621
TN228-J2-387-1226-1635-23-1599-003	NTWH2-D10	S.HILLS	SHELF	1599	0.21655	0.00138	12290	51.2	12265
TN228-J2-387-1226-1635-23-1599-004	NTWH2-D11	S.HILLS	SHELF	1599	0.21544	0.00155	12331	57.9	12318
TN228-J2-387-1226-1635-23-1599-005	NTWH2-D12-2	S.HILLS	SHELF	1599	0.19680	0.00138	13058	56.1	13041
TN228-J2-387-1226-0615-017-1748-001	NTWH2-E01	S.HILLS	SHELF	1748	0.18516	0.00164	13548	71.3	13502
TN228-J2-387-1226-0615-017-1748-002	NTWH2-E02	S.HILLS	SHELF	1748	0.21514	0.00136	12342	50.8	12341
TN228-J2-387-1226-0615-017-1748-004	NTWH2-E03	S.HILLS	SHELF	1748	0.14146	0.00138	15710	78.5	16911
TN228-J2-387-1226-0615-017-1748-005	NTWH2-E04	S.HILLS	SHELF	1748	0.19807	0.00141	13007	57.0	12997
TN228-J2-387-1226-0615-017-1748-007	NTWH2-E05	S.HILLS	SHELF	1748	0.19382	0.00163	13181	67.7	13184
TN228-J2-387-1226-0615-017-1748-008	NTWH2-E06	S.HILLS	SHELF	1748	0.20090	0.00147	12893	58.9	12863
TN228-J2-387-1226-0615-017-1748-009	NTWH2-E07	S.HILLS	SHELF	1748	0.18434	0.00162	13583	70.6	13540
TN228-J2-387-1226-0615-017-1748-010	NTWH2-E08	S.HILLS	SHELF	1748	0.18876	0.00136	13393	57.8	13348
TN228-J2-387-1226-0615-017-1748-011	NTWH2-E09	S.HILLS	SHELF	1748	0.14158	0.00138	15704	78.2	16907
TN228-J2-387-1226-0615-017-1748-012	NTWH2-E10	S.HILLS	SHELF	1748	0.20704	0.00135	12651	52.5	12648
TN228-J2-387-1225-0439-04-2004-001	NTWH2-E11	S.HILLS	SHELF	2004	0.76103	0.00232	2194	24.5	853
TN228-J2-387-1225-0439-04-2004-006	NTWH2-E16	S.HILLS	SHELF	2004	0.72050	0.00191	2633	21.3	1291
TN228-J2-387-1225-0439-04-2004-007	NTWH2-E17	S.HILLS	SHELF	2004	0.82296	0.00270	1565	26.4	388
TN228-J2-387-1225-0439-04-2004-009	NTWH2-E18	S.HILLS	SHELF	2004	0.82792	0.00203	1517	19.7	304
TN228-J2-387-1225-0439-04-2004-010	NTWH2-E19	S.HILLS	SHELF	2004	0.71407	0.00213	2705	24.0	1300
TN228-J2-387-1225-0439-04-2004-011	NTWH2-E20	S.HILLS	SHELF	2004	0.68165	0.00187	3079	22.0	1656
TN228-J2-387-1225-0147-02-2066-001	NTWH2-E21	S.HILLS	SHELF	2066	0.80666	0.00245	1726	24.4	515
TN228-J2-387-1225-0147-02-2066-007	NTWH2-E22	S.HILLS	SHELF	2066	0.79234	0.00228	1870	23.1	603
TN228-J2-387-1225-0147-02-2066-008	NTWH2-E23	S.HILLS	SHELF	2066	0.82858	0.00302	1511	29.3	304
TN228-J2-387-1225-0147-02-2066-009	NTWH2-E24	S.HILLS	SHELF	2066	0.74247	0.00193	2392	20.8	1015
TN228-J2-387-1225-0147-02-2066-010	NTWH2-E25	S.HILLS	SHELF	2066	0.76577	0.00190	2144	19.9	776
TN228-J2-387-1225-0147-02-2066-010	NTWH2-E25-2	S.HILLS	SHELF	2066	0.76488	0.00198	2153	20.8	828
TN228-J2-395-0113-0902-01-2193-005	NTWH2-E26	S.HILLS	SHELF	2193	0.82580	0.00238	1538	23.2	387
TN228-J2-395-0113-0902-01-2193-007	NTWH2-E27	S.HILLS	SHELF	2193	0.79738	0.00274	1819	27.6	587
TN228-J2-395-0113-1206-01-2193-025	NTWH2-E28	S.HILLS	SHELF	2193	0.81699	0.00200	1624	19.6	451
TN228-J2-393-0112-0124-06-1657-001	NTWH2-F01	KNOB	SOUTHWEST	1657	0.02998	0.00172	28173	459.9	30865
TN228-J2-393-0112-0124-06-1657-004	NTWH2-F04	KNOB	SOUTHWEST	1657	0.02648	0.00194	29172	590.0	31661

TN228-J2-393-0112-0124-06-1657-005	NTWH2-F05	KNOB	SOUTHWEST	1657	0.00559	0.00196	41666	2822.7	43787
TN228-J2-393-0112-0124-06-1657-005	NTWH2-F05-2	KNOB	SOUTHWEST	1657	0.00721	0.00196	39619	2184.7	42141
TN228-J2-393-0112-0124-06-1657-006	NTWH2-F06	KNOB	SOUTHWEST	1657	0.02191	0.00194	30693	711.2	33252
TN228-J2-393-0112-0124-06-1657-006	NTWH2-F06-2	KNOB	SOUTHWEST	1657	0.02184	0.00195	30717	715.3	33279
TN228-J2-393-0112-0124-06-1657-007	NTWH2-F07	KNOB	SOUTHWEST	1657	0.03680	0.00192	26528	419.3	29454
TN228-J2-393-0112-0124-06-1657-007	NTWH2-F07-2	KNOB	SOUTHWEST	1657	0.03751	0.00193	26374	413.1	29268
TN228-J2-393-0112-0124-06-1657-008	NTWH2-F08	KNOB	SOUTHWEST	1657	0.00310	0.00197	46407	5116.3	46152
TN228-J2-393-0112-0124-06-1657-008	NTWH2-F08-2	KNOB	SOUTHWEST	1657	0.00320	0.00197	46145	4933.6	46137
TN228-J2-393-0112-0124-06-1657-009	NTWH2-F09	KNOB	SOUTHWEST	1657	0.03762	0.00197	26350	419.9	29240
TN228-J2-393-0112-0124-06-1657-010	NTWH2-F10	KNOB	SOUTHWEST	1657	0.02443	0.00194	29817	637.1	32298
TN228-J2-393-0112-0124-06-1657-010	NTWH2-F10-2	KNOB	SOUTHWEST	1657	0.02471	0.00194	29725	629.6	32211
TN228-J2-390-1615-06-2170-001	NTWH2-F11	CASCADE	EAST	2170	0.83858	0.00240	1414	23.0	154
TN228-J2-390-1615-06-2170-002	NTWH2-F12	CASCADE	EAST	2170	0.82808	0.00315	1515	30.6	306
TN228-J2-390-1615-06-2170-003	NTWH2-F13	CASCADE	EAST	2170	0.78882	0.00198	1906	20.2	592
TN228-J2-390-1615-06-2170-004	NTWH2-F14	CASCADE	EAST	2170	0.82148	0.00204	1580	20.0	387
TN228-J2-390-1615-06-2170-005	NTWH2-F15	CASCADE	EAST	2170	0.83348	0.00207	1463	19.9	169
TN228-J2-390-0113-1145-04-2279-01	NTWH2-G01	CASCADE	EAST	2279	0.66330	0.00238	3298	28.8	1859
TN228-J2-390-0113-1145-04-2279-02	NTWH2-G02	CASCADE	EAST	2279	0.75802	0.00192	2226	20.4	861
TN228-J2-390-0113-1145-04-2279-03	NTWH2-G03	CASCADE	EAST	2279	0.84170	0.00242	1384	23.1	122
TN228-J2-390-0113-1145-04-2279-04	NTWH2-G04	CASCADE	EAST	2279	0.66213	0.00261	3312	31.6	2011
TN228-J2-390-0113-1145-04-2279-05	NTWH2-G05	CASCADE	EAST	2279	0.63580	0.00193	3638	24.4	2038
TN228-J2-390-0113-1145-04-2279-06	NTWH2-G06	CASCADE	EAST	2279	0.69538	0.00206	2918	23.8	1544
TN228-J2-390-0113-1145-04-2279-07	NTWH2-G07	CASCADE	EAST	2279	0.66156	0.00208	3319	25.2	2031
TN228-J2-390-0113-1145-04-2279-08	NTWH2-G08	CASCADE	EAST	2279	0.81743	0.00337	1619	33.1	403
TN228-J2-390-0113-1145-04-2279-09	NTWH2-G09	CASCADE	EAST	2279	0.75851	0.00253	2220	26.7	853
TN228-J2-390-0113-1145-04-2279-10	NTWH2-G10	CASCADE	EAST	2279	0.67662	0.00202	3138	24.0	1769
TN228-J2-390-0103-1024-03-2281-001	NTWH2-G11	CASCADE	EAST	2281	0.81717	0.00343	1622	33.7	431
TN228-J2-392-0110-1120-07-2341-001	NTWH2-G12	FINGER	SOUTHWEST	2341	0.80803	0.00236	1712	23.4	511
TN228-J2-392-0110-1120-07-2341-003	NTWH2-G14	FINGER	SOUTHWEST	2341	0.68843	0.00203	2999	23.6	1588
TN228-J2-392-0110-1120-07-2341-004	NTWH2-G15	FINGER	SOUTHWEST	2341	0.81484	0.00279	1645	27.5	444
TN228-J2-391-0109-0930-25-2386-001	NTWH2-G16	FRACTURE	SOUTHWEST	2386	0.77048	0.00250	2095	26.1	746
TN228-J2-391-0109-0930-25-2386-002	NTWH2-G17	FRACTURE	SOUTHWEST	2386	0.71227	0.00210	2726	23.7	1351
TN228-J2-391-0109-0930-25-2386-003	NTWH2-G18	FRACTURE	SOUTHWEST	2386	0.79833	0.00289	1809	29.1	551
TN228-J2-391-0109-0930-25-2386-004	NTWH2-G19	FRACTURE	SOUTHWEST	2386	0.72737	0.00213	2557	23.5	1176
TN228-J2-390-0103-0815-02-2395-001	NTWH2-G20	CASCADE	EAST	2395	0.75753	0.00220	2231	23.4	871
TN228-J2-390-0103-0815-02-2395-002	NTWH2-G21	CASCADE	EAST	2395	0.74585	0.00223	2356	24.1	1008
TN228-J2-390-0103-0815-02-2395-003	NTWH2-G22	CASCADE	EAST	2395	0.81010	0.00271	1692	26.9	503
TN228-J2-390-0103-0815-02-2395-004	NTWH2-G23	CASCADE	EAST	2395	0.74597	0.00229	2354	24.7	1001
TN228-J2-390-0103-0815-02-2395-005	NTWH2-G24	CASCADE	EAST	2395	0.76308	0.00228	2172	24.0	834
TN228-J2-390-0103-0815-02-2395-006	NTWH2-G25	CASCADE	EAST	2395	0.83515	0.00284	1447	27.3	180
TN228-J2-390-0103-0815-02-2395-007	NTWH2-G26	CASCADE	EAST	2395	0.73395	0.00235	2485	25.8	1108
TN228-J2-390-0103-0815-02-2395-008	NTWH2-G27	CASCADE	EAST	2395	0.77098	0.00235	2089	24.5	733
TN228-J2-390-0103-0815-02-2395-009	NTWH2-G28	CASCADE	EAST	2395	0.80558	0.00342	1737	34.1	518
TN228-J2-390-0103-0815-02-2395-010	NTWH2-G29	CASCADE	EAST	2395	0.75247	0.00230	2285	24.6	910
TN228-J2-389-0101-1024-10-1261-001	NTWH2-G30	EAST OF ST. HELENS	EAST	1261	0.76879	0.00227	2112	23.7	752
TN228-J2-389-0101-0930-07-1296-001	NTWH2-G31	EAST OF ST. HELENS	EAST	1296	0.84218	0.00245	1380	23.4	113
TN228-J2-393-0111-1851-2-1816-002	NTWH2-G32	KNOB	SOUTHWEST	1816	0.14756	0.00181	15371	98.5	16626
TN228-J2-393-0111-1851-2-1816-004	NTWH2-G33	KNOB	SOUTHWEST	1816	0.14108	0.00183	15732	103.9	16930
TN228-J2-393-0111-1851-2-1816-005	NTWH2-G34	KNOB	SOUTHWEST	1816	0.14652	0.00180	15428	98.5	16686
TN228-J2-393-0111-1851-2-1816-007	NTWH2-G35	KNOB	SOUTHWEST	1816	0.14539	0.00180	15490	99.5	16741
TN228-J2-393-0111-1851-2-1816-008	NTWH2-G36	KNOB	SOUTHWEST	1816	0.01621	0.00195	33111	965.6	35797
TN228-J2-393-0112-0730-13-1442-001	NTWH2-G37	KNOB	SOUTHWEST	1442	0.13937	0.00219	15830	126.1	17010
TN228-J2-389-0101-0732-04-1373-002	NTWH2-G38-2	EAST OF ST. HELENS	EAST	1373	0.46792	0.00189	6101	32.5	4428
TN228-J2-389-0101-0732-04-1373-005	NTWH2-G39	EAST OF ST. HELENS	EAST	1373	0.00930	0.00204	37572	1762.5	40346
TN228-J2-389-0101-0732-04-1373-006	NTWH2-G40	EAST OF ST. HELENS	EAST	1373	0.00611	0.00198	40956	2607.3	43209
TN228-J2-385-1221-0558-05-1060-006	NTWH2-H01	S.HILLS	SHELF	1060	0.44383	0.00230	6525	41.6	5797
TN228-J2-385-1221-0558-05-1060-007	NTWH2-H02	S.HILLS	SHELF	1060	0.45758	0.00224	6280	39.4	5597
TN228-J2-390-0103-1615-06-2170-006	NTWH2-H04-2	CASCADE	EAST	2170	0.82576	0.00260	1538	25.3	379
TN228-J2-390-0103-1615-06-2170-007	NTWH2-H05	CASCADE	EAST	2170	0.83090	0.00537	1488	51.9	275
TN228-J2-395-0113-0902-01-2193-010	NTWH2-H06-2	S.HILLS	SHELF	2193	0.81063	0.00234	1686	23.2	477
TN228-J2-395-0113-0902-01-2193-005	NTWH2-H07-2	S.HILLS	SHELF	2193	0.81692	0.00394	1624	38.7	432
TN228-J2-395-0113-0902-01-2193-007	NTWH2-H08-2	S.HILLS	SHELF	2193	0.79965	0.00234	1796	23.6	546
TN228-J2-395-0113-0902-01-2193-008	NTWH2-H09-2	S.HILLS	SHELF	2193	0.80049	0.00323	1788	32.4	523
TN228-J2-395-0113-0902-01-2193-009	NTWH2-H10	S.HILLS	SHELF	2193	0.82237	0.00245	1571	23.9	388
TN228-J2-395-0113-1206-01-2193-021	NTWH2-H11	S.HILLS	SHELF	2193	0.82236	0.00342	1571	33.4	389
TN228-J2-395-0113-1206-01-2193-022	NTWH2-H12	S.HILLS	SHELF	2193	0.78192	0.00250	1976	25.7	663
TN228-J2-395-0113-1206-01-2193-023	NTWH2-H13	S.HILLS	SHELF	2193	0.84364	0.00250	1366	23.8	113
TN228-J2-395-0113-1206-01-2193-024	NTWH2-H14	S.HILLS	SHELF	2193	0.79997	0.00313	1793	31.4	546
TN228-J2-395-0113-1206-01-2193-025	NTWH2-H15-2	S.HILLS	SHELF	2193	0.80749	0.00398	1718	39.6	513
TN228-J2-395-0113-1206-01-2193-026	NTWH2-H16	S.HILLS	SHELF	2193	0.80890	0.00242	1704	24.0	506
TN228-J2-395-0113-1206-01-2193-027	NTWH2-H17	S.HILLS	SHELF	2193	0.78927	0.00237	1901	24.1	595
TN228-J2-395-0113-1206-01-2193-028	NTWH2-H18	S.HILLS	SHELF	2193	0.78968	0.00238	1897	24.2	600
TN228-J2-395-0113-1206-01-2193-029	NTWH2-H19	S.HILLS	SHELF	2193	0.83370	0.00404	1461	38.9	181

TN228-J2-395-0113-1206-01-2193-030	NTWH2-H20	S.HILLS	SHELF	2193	0.74564	0.00259	2358	27.9	1009
TN228-J2-387-1226-1148-20-1680-009	NTWH2-H21	S.HILLS	SHELF	1680	0.22458	0.00256	11997	91.7	11681
TN228-J2-387-1226-1148-20-1680-010	NTWH2-H22	S.HILLS	SHELF	1680	0.19829	0.00185	12998	74.8	12985
TN228-J2-387-1226-1148-20-1680-07	NTWH2-H23	S.HILLS	SHELF	1680	0.22189	0.00176	12094	63.5	11889
TN228-J2-387-1226-1148-20-1680-06	NTWH2-H24	S.HILLS	SHELF	1680	0.20662	0.00181	12667	70.2	12662
TN228-J2-387-1226-1148-20-1680-08	NTWH2-H25	S.HILLS	SHELF	1680	0.20182	0.00227	12856	90.2	12836
TN228-J2-392-0110-1547-10-2217-001	NTWH2-H26	FINGER	SOUTHWEST	2217	0.81958	0.00299	1598	29.3	390
TN228-J2-387-1224-2355-1-2051-06	NTWH2-H27	S.HILLS	SHELF	2051	0.73908	0.00218	2429	23.7	1030
TN228-J2-395-0113-1530-03-2090-005	NTWH2-H28	S.HILLS	SHELF	2090	0.83102	0.00341	1487	32.9	192
TN228-J2-395-0113-1530-03-2090-006	NTWH2-H29	S.HILLS	SHELF	2090	0.82867	0.00304	1510	29.4	296
TN228-J2-395-0113-1530-03-2090-007	NTWH2-H30	S.HILLS	SHELF	2090	0.84171	0.00751	1384	71.6	144
TN228-J2-395-0113-1530-03-2090-008	NTWH2-H31	S.HILLS	SHELF	2090	0.83372	0.00720	1461	69.4	198
TN228-J2-395-0113-1530-03-2090-009	NTWH2-H32	S.HILLS	SHELF	2090	0.83247	0.00674	1473	65.1	198
TN228-J2-395-0113-1530-03-2090-010	NTWH2-H33	S.HILLS	SHELF	2090	0.83481	0.00230	1450	22.2	175
TN228-J2-392-0110-1409-08-2225-01	NTWH2-H34	FINGER	SOUTHWEST	2225	0.28613	0.00180	10052	50.6	9099
TN228-J2-392-0110-1409-08-2225-02	NTWH2-H35	FINGER	SOUTHWEST	2225	0.36428	0.00144	8112	31.7	7647
TN228-J2-392-0110-1409-08-2225-05	NTWH2-H36	FINGER	SOUTHWEST	2225	0.38679	0.00144	7630	30.0	6558
TN228-J2-392-0110-1409-08-2225-08	NTWH2-H37	FINGER	SOUTHWEST	2225	0.41798	0.00181	7007	34.8	6445
TN228-J2-392-0110-1409-08-2225-09	NTWH2-H38	FINGER	SOUTHWEST	2225	0.37604	0.00258	7857	55.1	7318
TN228-J2-387-1224-2355-1-2051-09	NTWH2-H39	S.HILLS	SHELF	2051	0.81933	0.00288	1601	28.2	393
TN228-J2-393-0112-0730-13-1442-007	NTWH2-H40	KNOB	SOUTHWEST	1442	0.24042	0.00173	11450	57.9	10913
TN228-J2-393-0112-0730-13-1442-008	NTWH2-H41	KNOB	SOUTHWEST	1442	0.25280	0.00183	11047	58.1	10323
TN228-J2-390-0104-0815-16-968-003	NTWH2-H42	CASCADE	EAST	968	0.00873	0.00190	38087	1745.0	40838
TN228-J2-390-0104-0815-16-968-004	NTWH2-H43	CASCADE	EAST	968	0.01452	0.00193	33998	1066.3	36746
TN228-J2-390-0104-0815-16-968-005	NTWH2-H44	CASCADE	EAST	968	0.02351	0.00186	30126	635.4	32592
TN228-J2-386-1223-1345-011-899-003	NTWH2-H45	S.HILLS	SHELF	899	0.89722	0.00253	871	22.6	80
TN228-J2-386-1223-1345-011-899-006	NTWH2-H46	S.HILLS	SHELF	899	0.87986	0.00184	1028	16.8	285
TN228-J2-386-1223-1345-011-899-010	NTWH2-H47	S.HILLS	SHELF	899	0.87880	0.00197	1038	18.1	291

Table 4.3-Statistical results of comparing different coral populations

Distribution 1	Distribution 2	Wilcoxon Test Results		Brown Forsythe	
		Rank Sum	p-values	F	p value
YD (NA)	20000-30000 (NA)	460.5	0.10500	35.9736	<e-4
YD (NA)	H1 (NA)	1331	0.95400	8.4929	0.0044
YD (NA)	ACR (SO)	814	0.04610	23.6922	<e-4
H1 (NA)	LGM (NA)	637.5	0.00012	28.8051	<e-4
H1 (NA)	ACR (SO)	854	0.00004	14.1331	0.003
LGM (NA)	ACR (SO)	504	0.35640	5.2879	0.026
20000-30000 (NA)	0-10000 (NA)	780	0.00000	1.4049	0.2421
20000-30000 (NA)	10000-20000 (NA)	1061.5	0.00570	36.3609	<e-4
20000-30000 (NA)	30000-40000 (NA)	693	0.07220	11.7331	0.0012
20000-30000 (NA)	40000-50000 (NA)	506	0.37360	49.0273	<e-4

Table 4.3 Wilcoxon and Brown-Forsythe test results for comparing depth distributions during different time periods in this study. North Atlantic distributions are indicated by (NA) and Southern Ocean distributions are indicated by (SO).

Table 3.4-U-Series and Libby Age of Antarctic Cold Reversal (ACR) Corals

Name of Coral	Seamount	Depth	Libby Age	U/Th date
ESA01	Shelf	1898	13089	14314
ESD04	Shelf	1947	12204	13649
NTWH2-E07	Shelf	1748	13583	15253
NTWH2-H41	Southwest	1442	11047	12374
ESI04	Shelf	1000	14342	16652
NTWH2-G37	Southwest	1442	15830	17850
NTWH2-D07	Shelf	1575	15995	17939
NTWH2-G33	Southwest	1816	15732	18253
NTWH2-G34	Southwest	1816	15428	17746
NTWH2-D12	Shelf	1599	13058	14639

Table 3.4: Reconnaissance 14C ages and U/Th ages of Southern Ocean corals from the ACR mode. These U/Th ages confirm that the mode seen in the Southern ocean data set is the ACR and not the YD or H1